

Supplementary Information for

Revealing the mechanisms of vesicle formation with multiple spectral methods

Jianhui Li^a, Shun-li Chen^b, Yi Hou^a, Qunhui Yuan^c, Wei Gan^{a,*}

^a Shenzhen Key Laboratory of Flexible Printed Electronics Technology, and School of Science, Harbin Institute of Technology (Shenzhen), University Town, Shenzhen 518055, Guangdong; School of Chemistry and Chemical Engineering, Harbin Institute of Technology, Harbin 150001, Heilongjiang, China.

E-mail: ganwei@hit.edu.cn

^b Department of Chemistry and Key Laboratory for Preparation and Application of Ordered Structure Materials of Guangdong Province, Shantou University, Shantou 515063, Guangdong, China.

^c Shenzhen Key Laboratory of Flexible Printed Electronics Technology, and School of Materials Science and Engineering, Harbin Institute of Technology (Shenzhen), University Town, Shenzhen 518055, Guangdong, China.

A. Figure S1 shows the time dependent SHG, TPF and Rayleigh spectra recorded in the formation of DOX/AOT vesicles at various concentrations.

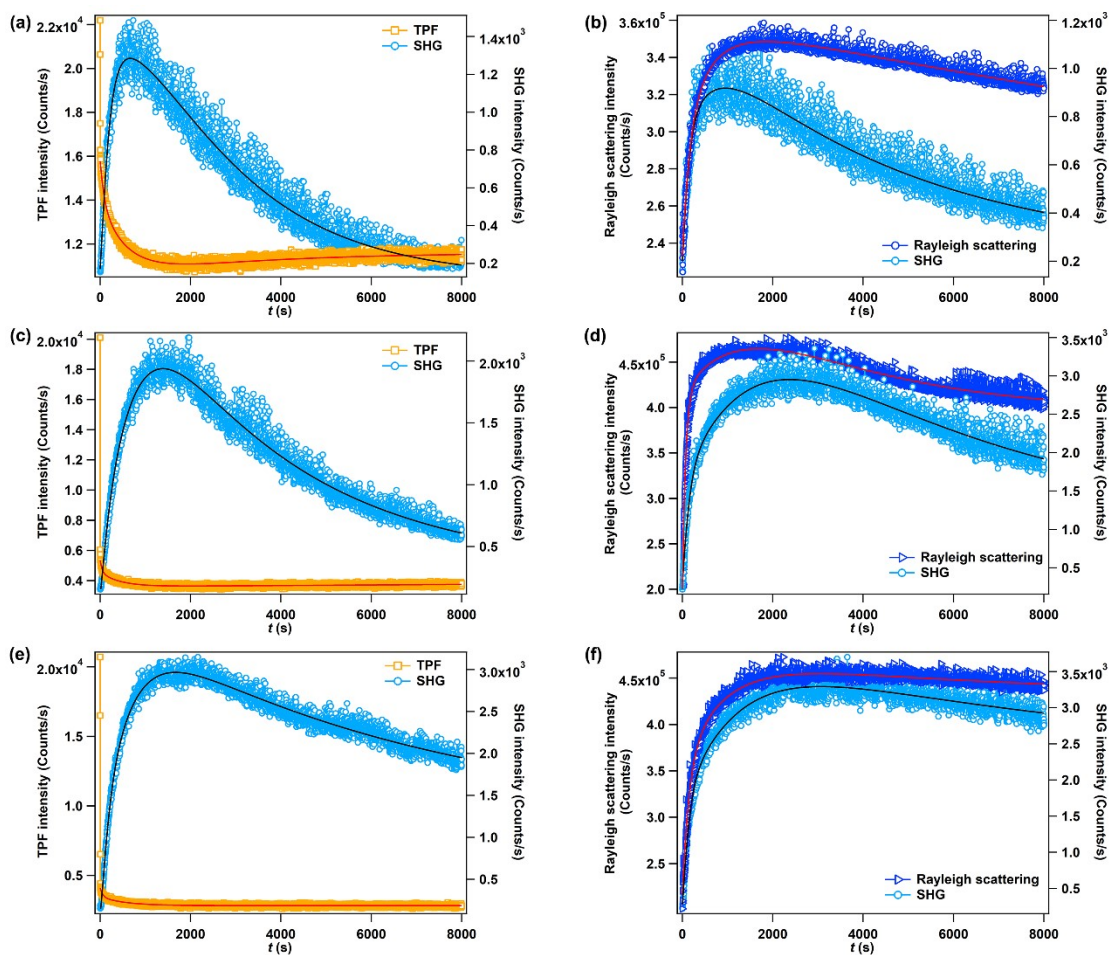


Figure S1. Simultaneously detected time-dependent curves of the TPF and SHG intensities after the rapid mixing of the DOX and AOT solutions (volume ratio 1:1) with the concentrations of 25/250 μM (a), 25/1000 μM (c), 25/2000 μM (e), respectively. Simultaneously detected time-dependent curves of the Rayleigh scattering and the SHG intensities after the rapid mixing of the DOX and AOT solutions with the concentrations of 25/250 μM (b), 25/1000 μM (d), 25/2000 μM (f), respectively.

B. Dynamic light scattering measurements

The size and zeta potential of the aggregates were characterized by dynamic light scattering equipment (Zetasizer Nano ZS90, Malvern) at the temperature set as 25 °C and the measurement direction as 90°. The laser wavelength was 633 nm. Although the size of the aggregated structures shown in Figure S2 fluctuated, their statistic average kept relatively stable both at different stages and under different AOT concentrations,

as measured by the DLS measurements (See Table S1). This observation shows that the AOT concentration has no significant effect on the average size of the vesicles. The forming of DOX/AOT vesicles also followed similar kinetics, as revealed by the dynamic change of the three optical scattering in Figure S1.

Table S1. The number mean diameters of the spontaneous vesicles/aggregates at different times and under different DOX/AOT concentration ratios

	DOX/AOT	25 μ M/250 μ M	25 μ M/500 μ M	25 μ M/1 mM	25 μ M/2 mM
Size (nm)	5 min	117 \pm 6	116 \pm 8	109 \pm 7	115 \pm 5
	10 min	121 \pm 2	109 \pm 4	114 \pm 4	111 \pm 7
	30 min	117 \pm 2	114 \pm 4	112 \pm 1	123 \pm 5
	60 min	122 \pm 7	116 \pm 4	112 \pm 3	118 \pm 7

C. The time constants obtained in fitting the SHG, TPF and Rayleigh scattering curves

Table S2. The time constants obtained in fitting the TPF and SHG curves shown in Figures 3 and S1. In some of the experiments, the change in the latter part of the TPF curves was too small to get a reliable fitting constant (marked by “/”).

	Time constant (s)	DOX/AOT (25 μ M/250 μ M)	DOX/AOT (25 μ M/500 μ M)	DOX/AOT (25 μ M/1000 μ M)	DOX/AOT (25 μ M/2000 μ M)
TPF	τ_1	88 \pm 4	54 \pm 3	41 \pm 2	56 \pm 3
	τ_2	557 \pm 14	423 \pm 10	436 \pm 11	557 \pm 10
	τ_3	3073 \pm 185	2768 \pm 177	/	/
SHG	τ_1	155 \pm 4	161 \pm 7	122 \pm 8	126 \pm 4
	τ_2	1489 \pm 362	906 \pm 81	649 \pm 14	577 \pm 12
	τ_3	2771 \pm 496	3927 \pm 238	5001 \pm 132	8786 \pm 420

Table S3. The time constants obtained in fitting the SHG and Rayleigh scattering curves shown in Figures 3 and S1.

	Time constant (s)	DOX/AOT (25 μ M/250 μ M)	DOX/AOT (25 μ M/500 μ M)	DOX/AOT (25 μ M/1000 μ M)	DOX/AOT (25 μ M/2000 μ M)
Rayleigh scattering	τ_1	182 \pm 4	229 \pm 4	70 \pm 1	145 \pm 3
	τ_2	837 \pm 40	1316 \pm 65	1438 \pm 128	865 \pm 27
	τ_3	9419 \pm 1080	6664 \pm 1190	2535 \pm 257	7421 \pm 1660

	τ_1	111±6	181±9	116±3	111±3
SHG	τ_2	623±56	1377±132	1572±116	1122±49
	τ_3	6542±450	2719±281	5600±879	8702±2300
